

Bailout Embeddings and Neutrally Buoyant Particles in Three-Dimensional Flows

Julyan H. E. Cartwright,^{1,*} Marcelo O. Magnasco,^{2,†} Oreste Piro,^{3,‡} and Idan Tuval.^{3,§}

¹*Laboratorio de Estudios Cristalográficos, CSIC, E-18071 Granada, Spain*

²*Mathematical Physics Lab, Rockefeller University, Box 212, 1230 York Avenue, NY 10021*

³*Institut Mediterrani d'Estudis Avançats, CSIC-UIB, E-07071 Palma de Mallorca, Spain*

(Dated: Published as Phys. Rev. Lett. **89**, 264501, 2002.)

We use the bailout embeddings of three-dimensional volume-preserving maps to study qualitatively the dynamics of small spherical neutrally buoyant impurities suspended in a time-periodic incompressible fluid flow. The accumulation of impurities in tubular vortical structures, the detachment of particles from fluid trajectories near hyperbolic invariant lines, and the formation of nontrivial three-dimensional structures in the distribution of particles are predicted.

PACS numbers: 05.45.Gg, 47.52.+j, 45.20.Jj

The dynamics of small spherical particles immersed in a fluid flow have received considerable attention in the past few years from both the theoretical and experimental points of view. On one hand, these particles are the simplest models for impurities whose transport in flows is of practical interest, and, on the other, their motion is governed by dynamical systems that even in the most minimal approximations display a rich and complex variety of behavior. When the density of the particles does not match that of the fluid, it is intuitively clear that the trajectories of a particle and of a fluid parcel will in general differ. This has been demonstrated in two-dimensional flows in which particles with density higher than the basic flow tend to migrate away from the parts of the flow dominated by rotation — in the case of chaotic flows, the KAM (Kolmogorov–Arnold–Moser) islands — while particles lighter than the fluid display the opposite tendency [1–3]. A more surprising result, however, is that neutrally buoyant particles may also detach from the fluid-parcel trajectories in the regions in which the flow is dominated by strain, to settle in the KAM islands [4]. The subtle dynamical mechanism responsible for the latter phenomenon has suggested a method to target KAM islands in Hamiltonian flows, and a recent generalization named a bailout embedding permits its extension to Hamiltonian maps as well [5].

Despite its obvious importance from the point of view of applications, the case in which the base flow is three-dimensional has been much less investigated. The probable reason for this is that very few simple realistic three-dimensional incompressible flow models exist. The few that are simple are not realistic — e.g., the ABC (Arnold–Beltrami–Childress) flow [6] — and those that are realistic are far more complex. In the study of the Lagrangian structure of three-dimensional incompressible time-periodic flows, where this difficulty is already present, the alternative approach of qualitatively modeling the flows by iterated three-dimensional volume-preserving (Liouvillian) maps has been successful in predicting fundamental structures later found both in more realistic theoretical flows and in experiments [7–10]. However, no similar approach has been followed to describe the motion of impurities in this kind of flow.

This Letter introduces the idea of bailout embeddings to

non-Hamiltonian systems. Two fundamentally unexplored problems are attacked with this new technique: firstly the investigation of generic structures of the dynamics of small particles in three-dimensional time-periodic flows, and secondly the study of the effects of noise and fluctuations on the dynamics of such particles, as well as the practical use of this analysis to reveal structures in three-dimensional flows that would be largely hidden to other methods. Regarding the former, we produce qualitative predictions using the bailout approach for maps that we confirm for flows. For the latter, we show that intricate but well defined structures may arise in a surprising way in the distribution of particles driven by extremely chaotic flows and the presence of noise. Bailout embedding is amenable to theoretical and experimental analysis in fluid dynamics, but the technique has many potential uses in the much broader community of physicists dealing in one way or another with nonlinear dynamical systems.

Let us first recall the equation of motion for a small, neutrally buoyant, spherical tracer in an incompressible fluid (the Maxey–Riley equation) [11, 12]. Under assumptions allowing us to retain just the Bernoulli, Stokes drag, and Taylor added mass contributions to the force exerted by the fluid on the sphere (the particle radius and its Reynolds number are small, as are the velocity gradients around it [4]), the equation of motion for the particle at position x is

$$\frac{d}{dt}(\dot{x} - u(x)) = -(\lambda + \nabla u) \cdot (\dot{x} - u(x)), \quad (1)$$

where \dot{x} represents the velocity of the particle, u that of the fluid, λ a number inversely proportional to the Stokes number of the particle — the ratio of the relaxation time of the particle back onto the fluid trajectories to the time scale of the flow — and ∇u the Jacobian derivative matrix of the flow. The difference between the particle velocity and the velocity of the surrounding fluid is exponentially damped with negative damping term $-(\lambda + \nabla u)$. In the case in which the flow gradients reach the magnitude of the viscous drag coefficient, there is the possibility that the Jacobian matrix ∇u may acquire an eigenvalue of positive real part in excess of the drag coefficient. If in these instances we can discard the time dependence of the eigenvectors it is clear that the trajec-

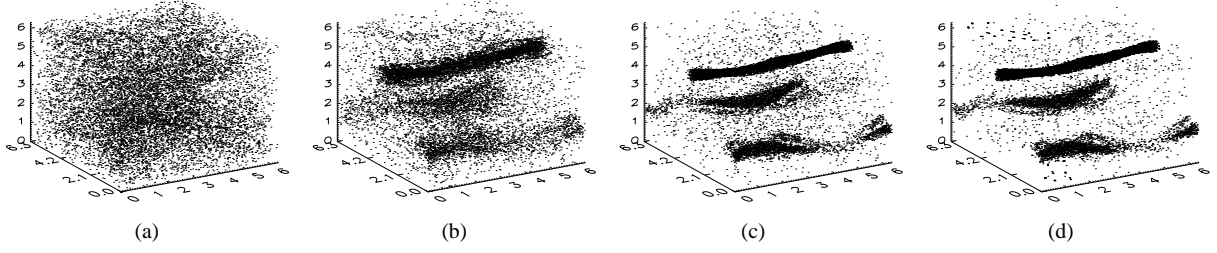


FIG. 1: For a homogeneous distribution of one hundred initial conditions we plot only the last 1000 steps of the map evolution for different values of λ : (a) $\lambda = 2$, (b) $\lambda = 1$, (c) $\lambda = 0.6$, (d) $\lambda = 0.5$. The images represent the $[0, 2\pi]$ cube in the phase space.

tories, instead of converging exponentially onto those defined by $\dot{\mathbf{x}} = \mathbf{u}$, may detach from them.

For incompressible two-dimensional flows, since the Jacobian matrix is traceless, the two eigenvalues must add up to zero, which implies that they are either both purely imaginary or both purely real, equal in absolute value and opposite in sign. The result is that the particles can abandon the fluid trajectories in the neighborhood of the saddle points and other unstable orbits, where the Jacobian eigenvalues are real, and eventually overcome the Stokes drag, to finally end up in a regular region of the flow on a KAM torus dominated by the imaginary eigenvalues. From a more physical point of view, this effect implies that the particles tend to stay away from the regions of strongest strain. In contrast to the two-dimensional case, in time-dependent three-dimensional flows the incompressibility condition only implies that the sum of the three independent eigenvalues must be zero. This less restrictive condition allows for many more combinations. Triplets of real eigenvalues, two positive and one negative or vice versa, as well as one real eigenvalue of either sign together with a complex-conjugate pair whose real part is of the opposite sign, are possible. Accordingly, chaotic trajectories may have one or two positive Lyapunov numbers, and a richer range of dynamical situations may be expected.

Instead of investigating all these in terms of a given fully fledged three-dimensional time-periodic model flow, we follow a qualitative approach based on iterated maps that roughly reproduces the properties of the impurity dynamics in a generic flow of this kind. In order to construct the map we first note that the dynamical system governing the behavior of neutrally buoyant particles is composed of some dynamics within another larger set of dynamics. Equation (1) can be seen as an equation for a variable $\delta = \dot{\mathbf{x}} - \mathbf{u}$ which in turn will define the equation of motion $\dot{\mathbf{x}} = \mathbf{u}$ of a fluid element whenever the solution of the former be zero. In this sense we may say that the fluid parcel dynamics is embedded in the particle dynamics. In reference to the fact that some of the embedding trajectories abandon some of those of the embedded dynamics, the generalization of this process is dubbed a bailout embedding [5].

It is rather easy to construct this type of embedding for map dynamics. Given a map $\mathbf{X}_{n+1} = \mathbf{T}(\mathbf{X}_n)$, a general bailout

embedding is given by

$$\mathbf{X}_{n+2} - \mathbf{T}(\mathbf{X}_{n+1}) = \mathbf{K}(\mathbf{X}_n) \cdot (\mathbf{X}_{n+1} - \mathbf{T}(\mathbf{X}_n)), \quad (2)$$

where $\mathbf{K}(\mathbf{X})$ is the bailout function whose properties determine which trajectories of the embedded map will be eventually abandoned by the embedding. The particular choice — naturally imposed by the particle dynamics — of the gradient as the bailout function in a flow translates in the map setting to

$$\mathbf{K}(\mathbf{x}) = e^{-\lambda} \cdot \nabla \mathbf{T}. \quad (3)$$

Bailout embeddings have been used to investigate targeting of KAM tori in Hamiltonian systems, as well as to explore generic properties of the distribution of small particles immersed in incompressible two-dimensional fluid flows [5], which are also of a Hamiltonian nature.

Here we consider the bailout embedding of a class of non-Hamiltonian systems: three-dimensional volume-preserving maps. In particular, we choose to represent qualitatively chaotic three-dimensional incompressible base flows that are periodic in time by ABC maps, a family

$$\mathbf{T} = \mathbf{T}_{ABC} : (x_n, y_n, z_n) \longrightarrow (x_{n+1}, y_{n+1}, z_{n+1}), \quad (4)$$

where

$$\begin{aligned} x_{n+1} &= x_n + A \sin z_n + C \cos y_n \pmod{2\pi}, \\ y_{n+1} &= y_n + B \sin x_{n+1} + A \cos z_n \pmod{2\pi}, \\ z_{n+1} &= z_n + C \sin y_{n+1} + B \cos x_{n+1} \pmod{2\pi}, \end{aligned} \quad (5)$$

that displays all the basic features of interest of the evolution of fluid flows. Depending on the parameter values, this map possesses two quasi-integrable behaviors: the one-action type, in which a KAM-type theorem exists, and with it invariant surfaces shaped as tubes or sheets; and the two-action type displaying the phenomenon of resonance-induced diffusion leading to global transport throughout phase space [7].

Let us now study the dynamics defined by Eqs (2)–(5). We first concentrate on the cases in which the flow is dominated by one-action behavior. In these we find an interesting generalization of the behavior already seen in two dimensions: particles are expelled from the chaotic regions to finally settle

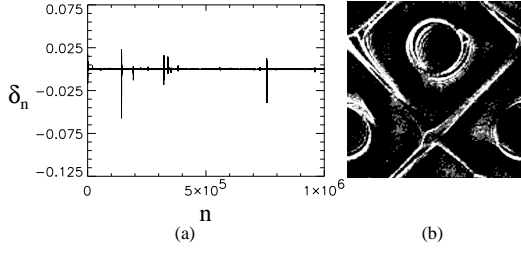


FIG. 2: (a) The evolution of one component of the difference δ_n between the particle and the fluid-flow velocities as a function of the number of iterations. (b) An xy slice of the phase space with those points where δ_n is greater than δ_0 . The square is the region $[0, 2\pi] \times [0, 2\pi]$.

in the regular KAM tubes. As an example, we take values of A , B , and C that lead to almost ergodic behavior of the fluid map: a single fluid trajectory almost completely covers the phase space. However, from randomly distributed initial conditions, the particle trajectories inevitably visit some hyperbolic regions where they detach from the corresponding fluid trajectory. In this fashion they find their way inside the invariant elliptic structures where they can finally relax back onto a safe fluid trajectory. In Fig. 1 we show how a homogeneous distribution of particles in the fluid flow, after a large number of stabilization iterations, finally settles inside the tubular KAM structures for different values of the parameter λ . When the value of λ decreases, more random trajectories follow this evolution: more particles fall into the invariant tubes.

In the two-action case, the eigenvalues of the Jacobian are very small on large portions of the trajectory, so that separation may only occur sporadically during the short time intervals in which the fluid parcel crosses the fast-motion resonances [7]. Most of the time, particles and fluid parcels follow exponentially convergent trajectories, causing the separations to be practically unobservable except for very small values of λ . Most probably, once the particles converge to the fluid dynamics, they remain attached. However, by adding a small amount of white noise, we can continually force the impurity to fluctuate around the flow trajectory [13]. From the application point of view, this noise may be considered to represent the effect of small scale turbulence, thermal fluctuations, etc., but here we use it only as a dynamical device. With this, the particles arrive in the neighborhood of the resonances with a non-negligible velocity mismatch with the fluid that is considerably amplified during the transit across the resonance. The measure of this mismatch is then a good detector of the proximity of the resonance.

Consider the following stochastic iterative system:

$$\mathbf{X}_{n+2} - \mathbf{T}(\mathbf{X}_{n+1}) = e^{-\lambda} \nabla \mathbf{T} \cdot (\mathbf{X}_{n+1} - \mathbf{T}(\mathbf{X}_n)) + \xi_n, \quad (6)$$

where the noise term ξ_n satisfies $\langle \xi_n \rangle = 0$, and $\langle \xi_n \xi_m \rangle = \varepsilon(1 - e^{-2\lambda}) \delta_{mn}$. We can recast Eq. (6) into

$$\mathbf{x}_{n+1} = \mathbf{T}(\mathbf{x}_n) + \delta_n,$$

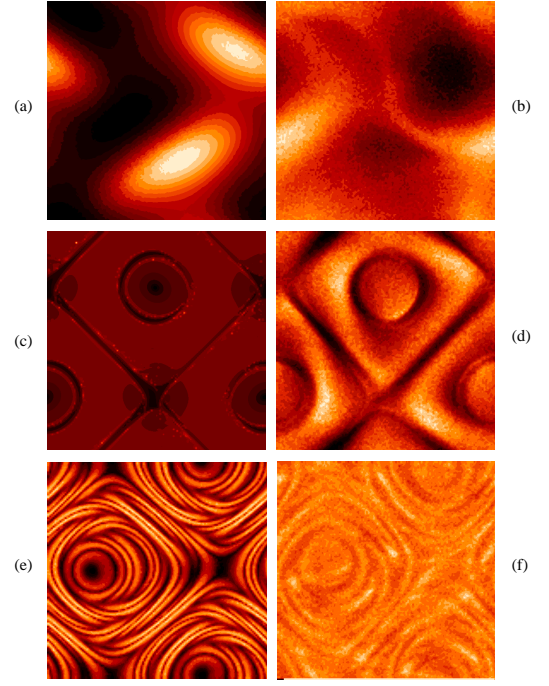


FIG. 3: The temperature amplitude — lighter is hotter — for the one-action, two-action and most chaotic cases ((a), (c), and (e) respectively), together with the corresponding slices of the impurity dynamics (histogram) in the phase space ((b), (d), and (f)). All images are the $[0, 2\pi] \times [0, 2\pi]$ region in the xy axis, for a slice in the z direction corresponding to the values $z \in [0, 0.49]$.

$$\delta_{n+1} = e^{-\lambda} \nabla \mathbf{T} \cdot \delta_n + \xi_n, \quad (7)$$

if we define the velocity separation between the fluid and the particle as $\delta_n = \mathbf{x}_{n+1} - \mathbf{T}(\mathbf{x}_n)$. We illustrate the behavior referred above by studying the most ergodic two-action case, in which all the fluid trajectories intersect the resonant lines. In Fig. 2a we show how δ_n grows strongly at some points, which correspond to the crossings of the resonant lines. In Fig. 2b we plot an xy slice of the three-dimensional cube, choosing those points where the value of δ_n is greater than a minimum value δ_0 . As shown, we recover the resonant structure previously noted [7, 8].

This is the most primitive way to obtain useful information from the noisy particle dynamics. A shrewder analysis [13] shows how the variance of the separation δ_n between particles and fluid trajectories and the variance of the noise ξ_n are related by a function that depends only on the particular point of the phase space that we look at, in a sort of temperature amplitude for the fluctuations of δ ,

$$\mathcal{T}(x) = \frac{\langle \delta^2 \rangle}{\langle \xi^2 \rangle} = \sum_{j=0}^{\infty} \left(e^{-j\lambda} \cdot \prod_{k=0}^j \nabla \mathbf{T} \big|_{\mathbf{T}^{-k}(x)} \right)^2. \quad (8)$$

This amplitude takes different values at different points of the flow. At those points that the particle dynamics tries to avoid,

its value increases, so the particle prefers to escape the hot regions and to fall into the cold ones.

In Fig. 3 we illustrate this phenomenon. First we analyze a one-action situation showing the temperature amplitude, as well as the impurity dynamics; Figs 3a and 3b respectively. Again we use slices of the three-dimensional cube to show the situation more clearly. Fig. 3a shows the temperature in a scaled color code. Fig. 3b shows a histogram of visits that a single particle pays to each bin of the space. The agreement between the higher-temperature regions and the less-visited ones is evident. Next we plot the same pictures but in the two-action case studied before; Figs 3c and 3d. Finally, we apply this analysis to a generic chaotic case where we do not have any information about the phase space structure. We show in Fig. 3e how the invariant manifolds are very twisted, and in Fig. 3f how the particles, even so, try to find the coldest regions of the flow.

In order to confirm that the above-described behavior is not an artefact of our mapping-based approach, we have performed analogous simulations using a continuous-time model as a base flow. We have considered neutrally buoyant particles immersed in a modified version of the ABC flow,

$$\begin{aligned}\dot{x} &= (1 + \sin 2\pi t) \cdot (A \sin z + C \cos y), \\ \dot{y} &= (1 + \sin 2\pi(t + 1/3)) \cdot (B \sin x + A \cos z), \\ \dot{z} &= (1 + \sin 2\pi(t + 2/3)) \cdot (C \sin y + B \cos x),\end{aligned}\quad (9)$$

in which each component of the velocity vector field is sinusoidally modulated with a relative phase shift of $2\pi/3$, and where x , y , and z are to be considered modulo 2π . While a detailed analysis of the dynamical aspects of this flow is beyond the scope of this Letter, we advance that it shows structures similar to those of the ABC maps, i.e., a complex array of KAM sheets and tubes surrounded by chaotic volumes. Neutrally buoyant particles evolved according to the true (simplified) Maxey–Riley equations, Eq. (1), based on this flow, show exactly the same tendency to accumulate inside KAM tubes as in the map case.

This application of bailout embedding is the first to be reported for a non-Hamiltonian dynamical system. Our approach can be pursued with two different goals in mind: on one hand, it contributes to the understanding of the physical behavior of impurities, and on the other, it provides a mathematical device to learn about the dynamical structures of the base flow in situations where these are very difficult to elu-

cidate directly. Both bodies of information are important to improve our presently scant knowledge of the transport properties of three-dimensional fluid flows.

This research was performed by IT as part of his doctoral thesis under the supervision of OP, together with additional input from JHEC and MOM. JHEC acknowledges the financial support of the Spanish CSIC, Plan Nacional del Espacio contract PNE-007/2000-C, MOM acknowledges the support of the Meyer Foundation, and OP and IT acknowledge the Spanish Ministerio de Ciencia y Tecnología, Proyecto CONOCE, contract BFM2000-1108 and Proyecto IMAGEN, contract REN2001-0802-C02-01.

* URL: <http://lec.ugr.es/~julyan>; Electronic address: julyan@lec.ugr.es

† URL: <http://asterion.rockefeller.edu/marcelo/>; Electronic address: marcelo@sur.rockefeller.edu

‡ URL: <http://www.imedeauib.es/~piro>; Electronic address: piro@imedeauib.es

§ URL: <http://www.imedeauib.es/~idan>; Electronic address: idan@imedeauib.es

- [1] A. Crisanti, M. Falcioni, A. Provenzale, and A. Vulpiani, *Phys. Lett. A* **150**, 79 (1990).
- [2] P. Tanga and A. Provenzale, *Physica D* **76**, 202 (1994).
- [3] A. Babiano, J. H. E. Cartwright, O. Piro, and A. Provenzale, in *Coherent Structures in Complex Systems*, edited by D. Reguera, L. Bonilla, and M. Rubi (Springer, 2001), vol. 567 of *Lecture Notes in Physics*, pp. 114–126.
- [4] A. Babiano, J. H. E. Cartwright, O. Piro, and A. Provenzale, *Phys. Rev. Lett.* **84**, 5764 (2000).
- [5] J. H. E. Cartwright, M. O. Magnasco, and O. Piro, *Phys. Rev. E* **65**, 045203(R) (2002).
- [6] T. Dombre, U. Frisch, J. M. Greene, M. Hénon, A. Mehr, and A. M. Soward, *J. Fluid Mech.* **167**, 353 (1986).
- [7] M. Feingold, L. P. Kadanoff, and O. Piro, *J. Stat. Phys.* **50**, 529 (1988).
- [8] O. Piro and M. Feingold, *Phys. Rev. Lett.* **61**, 1799 (1988).
- [9] J. H. E. Cartwright, M. Feingold, and O. Piro, *Phys. Rev. Lett.* **75**, 3669 (1995).
- [10] J. H. E. Cartwright, M. Feingold, and O. Piro, *J. Fluid Mech.* **316**, 259 (1996).
- [11] M. R. Maxey and J. J. Riley, *Phys. Fluids* **26**, 883 (1983).
- [12] E. E. Michaelides, *J. Fluids Eng.* **119**, 233 (1997).
- [13] J. H. E. Cartwright, M. O. Magnasco, and O. Piro, *Chaos* **12**, 489 (2002).